This is a post-peer-review, pre-copyedit version of an article published in **2018 25th International Workshop on Electric Drives: Optimization in Control of Electric Drives (IWED)**. The final authenticated version is available online at: https://doi.org/10.1109/IWED.2018.8321400

Impact of Low Switching-to-Fundamental Frequency Ratio on Predictive Current Control of PMSM

A simulation study

Leszek Jarzebowicz
Faculty of Electrical and Control Engineering
Gdansk University of Technology
Gdansk, Poland
leszek.jarzebowicz@pg.edu.pl

***Abstract*—Predictive current control algorithms for permanent magnet synchronous (PMSM) drives rely on an assumption that within short intervals motor currents can be approximated with linear functions. This approximation may result either from discretizing the motor model or from simplifications applied to the continuous-time model. As the linear current approximation has been recognized as inaccurate in case when the drive operates with low inverter's switching-to-fundamental frequency, it is expected that this inaccuracy affects precision of predictive control. This paper investigates the current prediction errors, related to the linear approximation, for an exemplary PMSM drive. Two methods are considered – a model based current prediction and a model-free algorithm. The analysis, carried out by simulation, reveals substantial errors that disqualify both considered prediction methods from applying them to drives operating with low switching-to-fundamental frequency ratio.**

Keywords—predictive control; permanent magnet synchronous motor; current sampling; modeling; high-speed drives; high-power drives

I. Introduction

Whilst new power electronic devices, like silicon carbide (SiC) and gallium nitride (GaN) transistors, appear to be a promising solution to increasing inverters' switching frequency, most present applications operate at a limited frequency – typically from a range between 500 Hz and 15 kHz. The lowest switching frequencies apply to high-power drives, where switching losses are a major concern [1].

On the other hand, there are low- and medium-power applications where power-to-weight and power-to-volume ratios are important. A common approach to improve these ratios is to extend the motor rotational speed range [2]. Such a trend can be noticed e.g. in electric and hybrid cars, where maximal speed of traction electric motors has been increased over the last years, and nowadays often substantially exceeds 10000 rpm [3].

Both limiting the switching frequency and extending the rotational speed leads to a low ratio between the switching frequency and the fundamental frequency of inverter output voltage (shortly referred to as "switching-to-fundamental frequency ratio"). In some applications this ratio can drop down below a value of 10 [1], and – as it has been recently acknowledged [4] – such operating conditions lead to substantial errors in linear approximation of motor currents, which is used to model the currents within short intervals. Since the linear approximation is commonly adopted in contemporary current sampling techniques [5], predictive control algorithms [6][7] and current ripples minimization [8], it is important to investigate the errors it causes under drive's low switching-to-fundamental frequency ratio operation.

This paper focuses on the impact of low switching-to-fundamental frequency ratio on current prediction errors in a permanent magnet synchronous (PMSM) drive that uses a regular two-level voltage source inverter. Two prediction methods are considered – a model-based method and a model-free method. The errors are derived for an exemplary non-salient high-speed PMSM drive with the minimal switching-to-fundamental frequency ratio of 14. The analysis is carried out using a hybrid continuous-discrete simulation model, which was validated in a previous paper [4].

II. Concerns of Modeling Currents Under Low Switching-to-Fundamental Frequency Operation

Generally, the waveforms of motor currents are precisely modeled using a differential equation, which can be formulated for different reference frames. For the rotating *d-q* frame, this equation can be written in vector notation as follows:

$$\frac{d\mathbf{i}}{dt} = \frac{1}{L}\left(-R\mathbf{i} - \mathbf{j}\omega L\mathbf{i} - \mathbf{j}\omega\psi_f + \mathbf{u}\right) \tag{1}$$

where: $\mathbf{i} = [i_d\ i_q]^T$ and $\mathbf{u} = [u_d\ u_q]^T$ represent current and voltage vectors in *d-q* coordinates; $L = L_d = L_q$ and R are stator inductance and resistance, respectively; ψ_f is flux linkage produced by the permanent magnets; ω is rotor (electrical) speed.

When analyzing short intervals, e.g. a single current control cycle, the model (1) is often simplified [9]. Typically, the resistive drop $R\mathbf{i}$ is neglected, which leads to a constant value

of $d\mathbf{i}/dt$ under steady supplying voltage $\mathbf{u}$. Consequently, the waveforms of motor currents are approximated by a set of linear functions derived individually for each steady-voltage interval, e.g. voltage modulation subinterval. In most cases, such an approximation is in agreement with the true current waveform. An example of experimentally recorded phase current waveform, which can be well approximated with a set of linear functions, is presented in Fig. 1a.

The linear approximation may also result simply from discretizing (1), which is necessary to implement the model in a digital controller. The discretization interval is usually equal to the control period T, which is assumed short enough for the linear approximation of current. Consequently, the current waveform within T is approximated with a linear function.

Some of predictive control methods use voltage modulation to obtain an infinite set of control outputs. In such a case, the current waveform within a control cycle is compound (as in Fig. 1a), because it consists of ripples, which are a response to subsequent voltages applied by the inverter. In order to simplify the control algorithm, the motor model reflects only a fundamental component of the current [9]. This component is a theoretical motor's response to a constant voltage, which value is equal to the mean of the modulated one. For symmetrical modulation methods, e.g. Space Vector Pulse Width Modulation (SV-PWM), the fundamental component is equal to the compound current waveform in the middle and at the margins of the control cycle. Similar to modeling the modulation-related transients, the fundamental component is assumed to be well represented within a control cycle by a linear function (as in Fig. 1a).

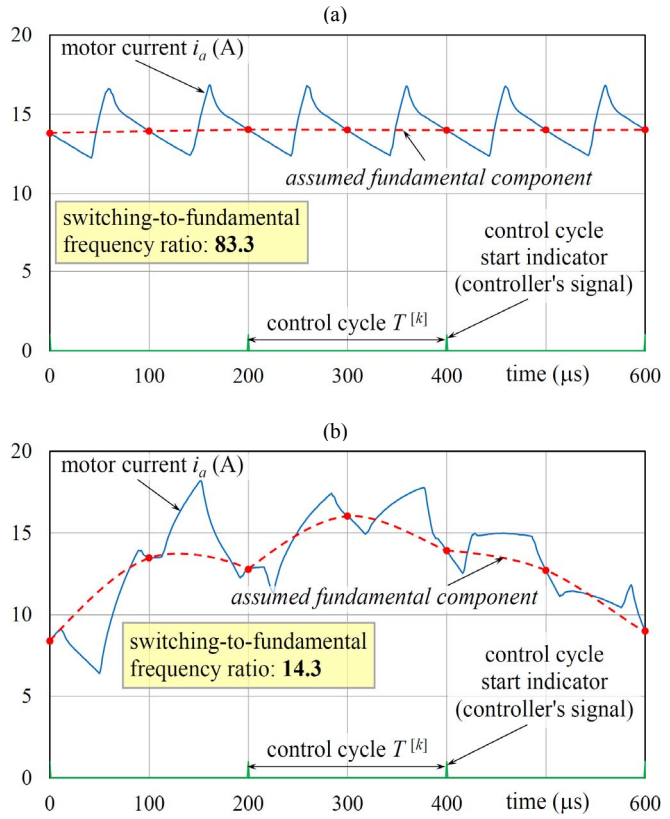

Fig. 1. PMSM phase current i_a waveforms recorded in laboratory drive operating with switching frequency of 5 kHz: (a) at 380 rad/s; (b) at 2200 rad/s

The linear approximation is well justified in most drives, where the switching-to-fundamental frequency ratio is high. However, operating with the low ratio makes the current change in an evidently nonlinear manner, as presented in Fig. 1b. This nonlinearity is most clearly observable for the fundamental component, where the function that crosses the compound current waveform in the middle and at both margins of control cycle cannot be linear.

The considered current nonlinearity is related to fast changes in rotor position, which cause that the rotor covers substantial angular distance $\Delta\theta$ during a single control cycle T. For instance, when a drive operates with the switching-to-fundamental frequency ratio of 14, the angular distance is $\Delta\theta \cong 25°$, and this causes substantial changes in d- and q-components of the voltage vector $\mathbf{u}$, even if the stationary components of this voltage do not change. Consequently, the assumption of constant $\mathbf{u}$ does not hold. The mechanism of influencing motor currents by the rotor movement was explained in detail in [4].

III. Considered Predictive Current Control Methods

To obtain versatile results, two utterly different current prediction methods are considered in the study. The first method is based on a mathematical model of the motor and the second one is an example of model-free prediction algorithm.

A. Model-based current prediction method

Motor mathematical model, which is used to predict the currents, originates from (1). Forward Euler approximation is applied to discretize the model with the discretization step equal to the control period T [6][7]:

$$\frac{d\mathbf{i}}{dt} \cong \frac{\mathbf{i}^{[k+1]} - \mathbf{i}^{[k]}}{T^{[k]}} \tag{3}$$

Consequently, the predicted current is computed as:

$$\mathbf{i}^{*[k+1]} = \mathbf{i}^{[k]} + \frac{T^{[k]}\left(\mathbf{u}^{[k]} - R\mathbf{i}^{[k]} - \mathbf{j}L\omega^{[k]}\mathbf{i}^{[k]} - \mathbf{j}\omega^{[k]}\psi_f\right)}{L} \tag{4}$$

The above equation consists of constants, which are related to motor parameters, as well as discrete variables, whose values are collected in a manner discussed below.

The timing scheme of the model-based prediction is presented in Fig. 2. In practice, current predictive control algorithm computes a set of predicted currents $\mathbf{i}^{*[k+1]}$, where each current is a response to different supplying voltage $\mathbf{u}^{[k]}$. This enables the control algorithm to select the optimal supplying vector according to a predefined criterion. In Finite Control Set (FCS) predictive methods, this voltage can be selected only from a set of seven fundamental vectors related to the possible states of inverter's transistors. In contrast, in

Continuous Control Set (CCS) methods this set is not limited, as modulated voltages can be applied to the motor. In both cases, the voltage $\mathbf{u}^{[k]}$ for any particular current prediction is assumed *a priori*, so it does not introduce any timing constraints.

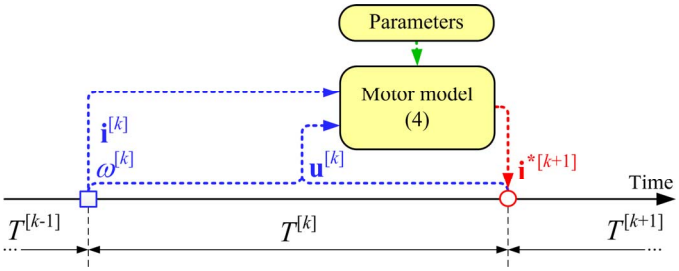

Fig. 2. Timing scheme of input data sampling and current prediction for the model-based method

In contrast, the discrete values of current $\mathbf{i}^{[k]}$ and speed $\omega^{[k]}$ included in (4) relate to measured values. However, they cannot be directly sampled at the beginning of control cycle $T^{[k]}$, because the selection of optimal $\mathbf{u}^{[k]}$ has to be done in advance to this instant. Thus, in practice, earlier measurements in combination with various delay compensation algorithms are used to compute $\mathbf{i}^{[k]}$ and $\omega^{[k]}$ [10]. Despite this practical problem, this simulation study assumes that the values $\mathbf{i}^{[k]}$ and $\omega^{[k]}$ are sampled at the beginning of $T^{[k]}$. This enables the investigation of the errors related solely to current prediction, without an impact of inaccurate delay compensation.

B. Model-free current prediction method

Model-free methods do not use any motor parameter, what makes them robust to parameters uncertainties and variations. The method considered in this paper was proposed in [11], but similar solutions can be also found in other papers, e.g. [12].

The considered method requires the use of a symmetric voltage modulation method and sampling motor currents twice per control cycle – at its beginning and in the middle (Fig. 3). Using the linear current approximation, the value of motor current $\mathbf{i}^{*[k+1]}$ for the beginning of next control cycle is predicted based on extrapolating a linear interpolant between the two current samples acquired within the control cycle $T_{[k]}$:

$$\mathbf{i}^{*[k+1]} = 2 \cdot \mathbf{i}_{mid}{}^{[k]} - \mathbf{i}^{[k]} \tag{5}$$

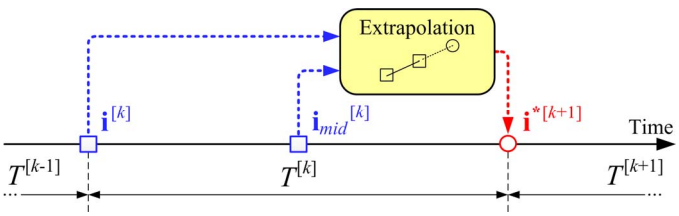

Fig. 3. Timing scheme of input data sampling and current prediction for the model-free method

The predicted current corresponds to the instant, which is only half a control cycle ahead of the last measurement required for prediction, but it was proven that such an approach combined with regular Field Oriented Control (FOC) [13] provides excellent dynamic control properties.

IV. Simulation Model

The simulation model corresponds to a laboratory drive consisting of: a PMSM, a 2-level inverter and a controller based on a digital signal processor. Parameters of this drive are included in Table I. The drive operates with constant control (PWM) frequency of $f = 1/T = 5$ kHz; the maximum speed equals 2200 rad/s. At this speed, the switching-to-fundamental frequency ratio approaches 14.

TABLE I. PMSM Drive Parameters

Parameter	Value
Control (PWM) cycle duration T	200 µs
Rated phase current amplitude I_r	15 A
DC-bus voltage U_{DC}	300 V
Rated speed (electrical) ω	2200 rad/s
Stator resistance R	0.1 Ω
Stator inductance L	1 mH
Permanent magnets flux linkage ψ_f	75 mWb

The two considered prediction algorithms are expected to provide results featured by different errors. Using the erroneous results as a control feedback would force the drive to operate differently for two considered predictive methods. This, in turn, would make deriving the two errors for the same operating conditions impossible. Therefore, the motor is controlled independently, based on FOC [14], and the prediction algorithm runs independently. Such an approach enables comparing the errors related to both considered prediction algorithms for the same operating conditions, as the errors do not change the control parameters.

In case of the model-based method, in order to exclude the impact of delay compensation algorithm on the predicted currents, the input values $\mathbf{i}^{[k]}$ and $\omega^{[k]}$ are directly sampled at the beginning of $T^{[k]}$, what makes the compensation algorithm redundant. Moreover, the prediction is made based on a reference voltage set by FOC for the forthcoming control cycle, which enables deriving errors between predicted and real current.

General structure of the model is shown in Fig. 4. The model is implemented in MATLAB/Simulink. For simplicity, only the fundamental current component is reflected in the model, as it was proven that such an approach reflects the errors related to non-linear current waveforms properly [4].

The upper part of the diagram consists of the motor, inverter and controller with implemented FOC algorithm. The motor is modeled based on continuous equation (1), complemented with reference frame transforms. In contrast, the controller and inverter are modeled using triggered subsystems,

which are executed upon occurrence of a defined slope of clocking signal *clk*. The clocking signal, shown in the upper right corner of Fig. 4, is a 5-kHz square wave, with rising slopes corresponding to beginning of control cycles and falling slope indicating midpoints of the cycles. The FOC algorithm is executed upon a falling slope, which means that it samples the inputs and updates the voltage reference in the middle of control cycle (processing time is not reflected in the model).

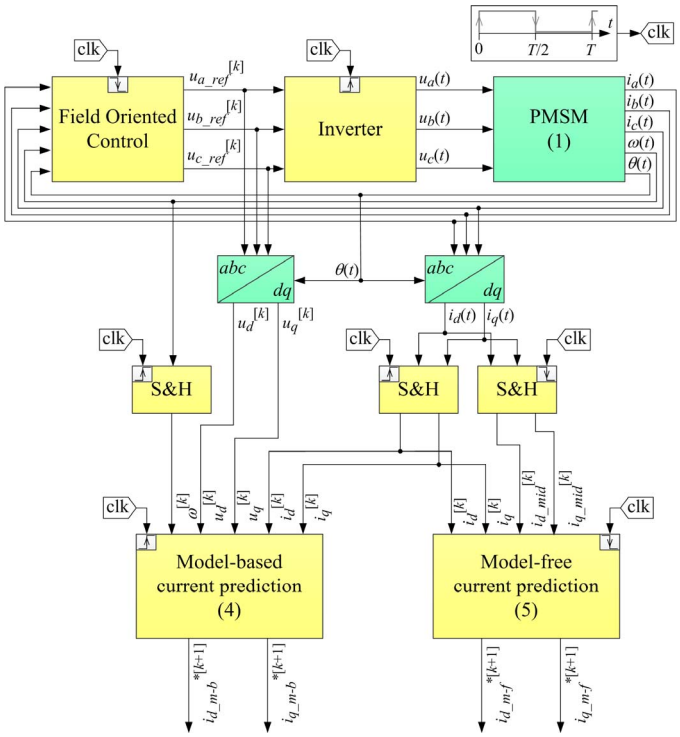

Fig. 4. General structure of simulation model

The inverter's model is executed at the beginning of control cycle, thus it updates the output voltages at this instant and holds them until the next execution. This way the motor voltages are constant within a control cycle and equal to the reference values. These properties enable modeling of the fundamental components of motor currents.

The lower part of Fig. 4 involves computations related to the current prediction methods. Continuous motor currents and discrete reference voltages are transformed into the *d-q* reference frame. Next, the currents are sampled at the beginning and in the middle of the control cycle, where the latter sample is required only by the model-free method. Additionally, motor speed, which is necessary only for the model-based method, is sampled at the beginning of the cycle. The discrete feedback is delivered to the prediction algorithms.

The model-based prediction is executed at the beginning of the control cycle; it predicts the *d-q* currents $i_{d\_m\text{-}b}{}^{*[k+1]}$ and $i_{q\_m\text{-}b}{}^{*[k+1]}$ with one-cycle prediction horizon. The model-free method runs in the middle of control cycle, and predicts the *d-q* currents $i_{d\_m\text{-}f}{}^{*[k+1]}$ and $i_{q\_m\text{-}f}{}^{*[k+1]}$ half a cycle ahead.

V. Simulation Results

The simulation study aims at investigating current prediction errors, related to operating with low switching-to-fundamental frequency ratio, for the PMSM drive whose parameters were given in the previous section. Deriving the maximal errors is the main concern, but it is desirable to also investigate a co-relation between the errors and drive's operating conditions.

The test scenario consists of accelerating from standstill to the rated speed, but first the results covering the last millisecond of the test are presented in Fig. 5. They correspond to operating at a steady speed of the rated value, i.e. to operating with the lowest switching-to-fundamental frequency ratio. The continuous waveforms of currents i_d and i_q are clearly not linear. Consequently, discrete values of the currents predicted using the model-based ($i_{d\_m\text{-}b}{}^*$, $i_{q\_m\text{-}b}{}^*$) and model-free method ($i_{d\_m\text{-}f}{}^*$, $i_{q\_m\text{-}f}{}^*$) substantially differ from the true values at the corresponding instants. The consequences of current linear approximation, used in the prediction algorithms, are graphically presented with dotted lines, for each method separately. The model-based method computes the current derivative based on the discrete feedback corresponding to the start-point of control cycle. Due to the continuous changes in the true derivative, the value of current predicted for the beginning of next control cycle differs from the true value by $\Delta i_{d\_m\text{-}b}{}^*$ or $\Delta i_{q\_m\text{-}b}{}^*$ for *d*- or *q*- current, respectively. The model-free method, which extrapolates the interplant between current samples acquired at the beginning and in the midpoint of control cycle, also features distinctive errors marked as $\Delta i_{d\_m\text{-}f}{}^*$ and $\Delta i_{q\_m\text{-}f}{}^*$ for *d*- and *q*- current, respectively.

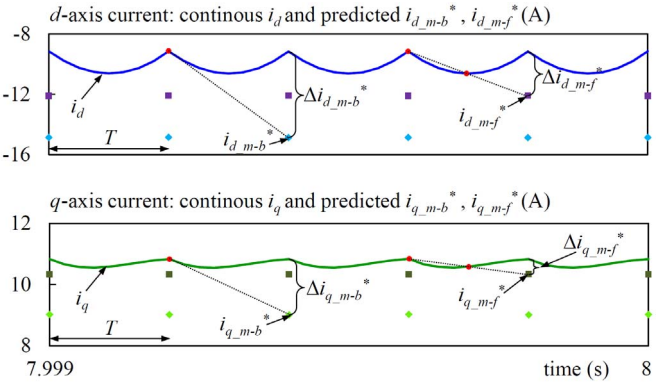

Fig. 5. Simulation results for operating at rated speed of 2200 rad/s (switching-to-fundamental frequency ratio of 14)

The results covering the whole simulation time are included in Fig. 6. During acceleration, the drive operates at current limitation (constant amplitude of i_a), generating the maximal available torque. Additionally, at $t \cong 5$ s the drive reaches the inverter's output voltage limit and switches into flux weakening operation, which requires negative i_d current. The i_q is then decreased to follow the inverter's current limitation. The errors of current prediction are drawn in two bottom subfigures of Fig. 6, separately for model-based and model-free method.

All four errors appear to gain with the increase of drive's speed. This speed-related gain is weakened by the decrease in i_q current, which starts at $t \cong 5$ s. This applies to both *d*- and *q*-current prediction errors, although the modulus of i_d increases with speed. Thus, it can be concluded that the absolute errors are mostly influenced by the switching-to-fundamental frequency ratio and by the i_q current.

In both predictive algorithms, the errors of *d*-axis current prediction are multiple times higher than that of *q*-axis. For model-based method the maximal *d*-axis prediction error is $max(\Delta i_{d\_m\text{-}b}^{*}) = 5.8$ A, which is nearly 40% of the rated current. The maximal *d*-axis prediction error for model-free method is lower $max(\Delta i_{d\_m\text{-}f}^{*}) = 3.0$ A, but still substantial compared with the rated current.

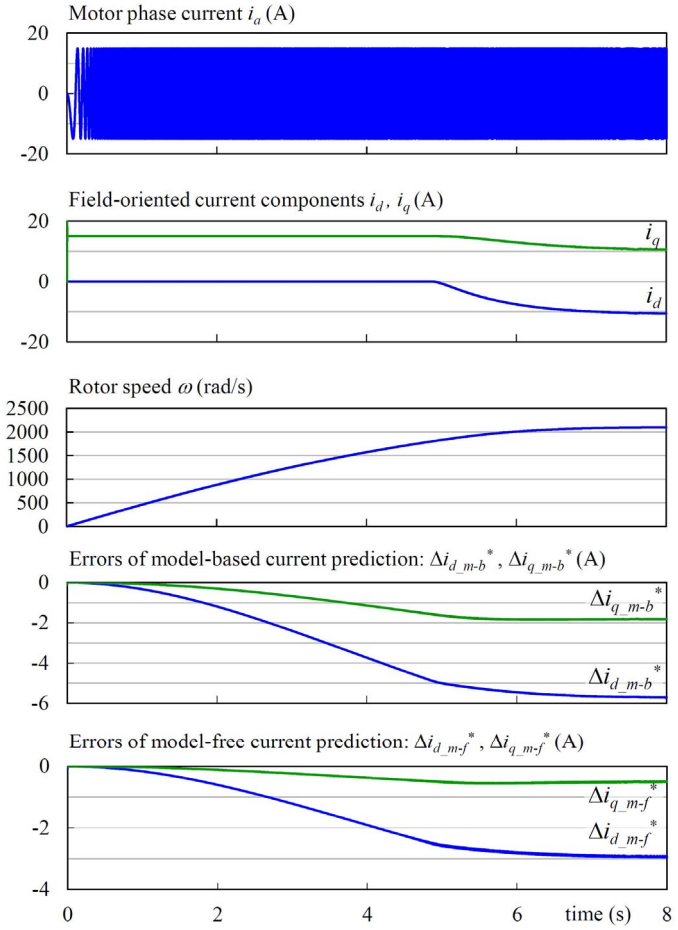

Fig. 6. Simulation results for accelerating from standstill to the rated speed

VI. Conclusion

The study proves that both considered current prediction methods provide erroneous outcomes when applied to a drive operating with low switching-to-fundamental frequency ratio. To the best of author's knowledge, this problem has not been identified before in research on predictive control.

The errors influence mostly the *d*-axis current component, thus they are expected to affect mostly the flux control. Both model-based and model-free prediction methods provide results which are deteriorated by low switching-to-fundamental frequency ratio, but the errors for the model-based method are higher, reaching 40% of the rated current. The derived errors disqualify the considered prediction methods from applying them to drives operating with low switching-to-fundamental frequency ratio. Such an application demands research on a new approach to modeling non-linear motor currents, applicable to digital controllers.

The parameter setup used in the study correspond to the switching-to-fundamental frequency ratio of 14, but the references report on applications featured by even lower ratios, where the prediction errors can potentially be much higher.

References

[1] S. K. Sahoo and T. Bhattacharya, "Rotor Flux-Oriented Control of Induction Motor With Synchronized Sinusoidal PWM for Traction Application," *IEEE Transactions on Power Electronics*, vol. 31, no. 6, pp. 4429–4439, Jun. 2016.

[2] M. D. and P. Winzer, "Shut Up About the Batteries: The Key to a Better Electric Car Is a Lighter Motor," *IEEE Spectrum: Technology, Engineering, and Science News*, 22-Jun-2017. [Online]. [3] K. H. Nam, *AC Motor Control and Electrical Vehicle Applications*, 1 edition. CRC Press, 2010.

[4] L. Jarzebowicz, "Errors of a Linear Current Approximation in High-Speed PMSM Drives," *IEEE Transactions on Power Electronics*, vol. 32, no. 11, pp. 8254–8257, Nov. 2017.

[5] J. Böcker and O. Buchholz, "Can oversampling improve the dynamics of PWM controls?," in *Industrial Technology (ICIT), 2013 IEEE International Conference on*, 2013, pp. 1818–1824.

[6] P. Cortes, J. Rodriguez, C. Silva, and A. Flores, "Delay Compensation in Model Predictive Current Control of a Three-Phase Inverter," *IEEE Transactions on Industrial Electronics*, vol. 59, no. 2, pp. 1323–1325, Feb. 2012.

[7] Y. Wang *et al.*, "Deadbeat Model-Predictive Torque Control With Discrete Space-Vector Modulation for PMSM Drives," *IEEE Transactions on Industrial Electronics*, vol. 64, no. 5, pp. 3537–3547, May 2017.

[8] P. Cervellini, P. Antoszczuk, R. G. Retegui, and M. Funes, "Current Ripple Amplitude Measurement in Multiphase Power Converters," *IEEE Transactions on Power Electronics*, vol. 32, no. 9, pp. 6684–6688, Sep. 2017.

[9] E. Persson, "Motor current measurement using time-modulated signals," in *Power Conversion Conference, 2002. PCC Osaka 2002. Proceedings of the*, 2002, vol. 2, pp. 716–720.

[10] T. Tarczewski and L. M. Grzesiak, "Constrained State Feedback Speed Control of PMSM Based on Model Predictive Approach," *IEEE Transactions on Industrial Electronics*, vol. 63, no. 6, pp. 3867–3875, Jun. 2016.

[11] L. Jarzebowicz, A. Opalinski, and M. Cisek, "Improving Control Dynamics of PMSM Drive by Estimating Zero-Delay Current Value," *Elektronika ir Elektrotechnika*, vol. 21, no. 2, Apr. 2015.

[12] A. Anuchin and V. Kozachenko, "Current loop dead-beat control with the digital PI-controller," in *2014 16th European Conference on Power Electronics and Applications (EPE'14-ECCE Europe)*, 2014, pp. 1–8.

[13] K. Urbanski, "A new sensorless speed control structure for PMSM using reference model," *Bulletin of the Polish Academy of Sciences Technical Sciences*, vol. 65, no. 4, pp. 489–496, 2017.

[14] L. Jarzebowicz, K. Karwowski, and W. J. Kulesza, "Sensorless algorithm for sustaining controllability of IPMSM drive in electric vehicle after resolver fault," *Control Engineering Practice*, vol. 58, pp. 117–126, Jan. 2017.